

Infrared optical Properties of $\text{La}_{0.7}\text{Ca}_{0.3}\text{MnO}_3$ Epitaxial Films

A. V. Boris^{1*}, N. N. Kovaleva¹, A. V. Bazhenov¹, A. V. Samoilov², N.-C. Yeh², and R. P.

Vasquez³

¹*Institute of Solid State Physics, Russian Academy of Sciences,*

Chernogolovka, Moscow (Dist., 142432, Russia

²*Department of Physics, California Institute of Technology, Pasadena, CA 91125, USA*

³*Jet Propulsion Laboratory, California Institute of Technology, Pasadena, CA 91109, USA*

Abstract

The reflectance of $\text{La}_{0.7}\text{Ca}_{0.3}\text{MnO}_3$ epitaxial thin films on perovskite substrates with a range of lattice constants is studied in the frequency range 50 cm^{-1} – 5000 cm^{-1} . The complex dielectric functions of the bare $\text{La}_{0.7}\text{Ca}_{0.3}\text{MnO}_3$ films are obtained by modeling the measured reflectivity spectra of the two-layer $\text{La}_{0.7}\text{Ca}_{0.3}\text{MnO}_3$ /substrate system with separately measured dielectric functions of the bare substrate. The results thus derived indicate that the transverse optical phonon modes of $\text{La}_{0.7}\text{Ca}_{0.3}\text{MnO}_3$ are strongly affected by the substrate-induced lattice distortion.

The origin of the colossal negative magnetoresistance (CMR) recently observed in perovskite manganites $\text{La}_{1-x}\text{A}_x\text{MnO}_3$ (A: divalent alkaline ions) have been a subject of intense experimental and theoretical studies. Recent theoretical investigations [1] have revealed that the lattice effects and the strong electron-phonon interaction due to the Jahn-Teller coupling play an important role in the occurrence of the CMR in manganites. Many aspects of the magnetic and resistivity data [2-5] can be successfully explained in terms of the scenario of lattice polaron conduction. In order to further verify the mechanism of the CMR effect and the correlation of lattice distortion with the magnetic and transport properties, infrared data are needed for providing direct information of the optical phonon modes and the electron-phonon interaction.

The investigations of the electrical transport and magnetic properties of $\text{La}_{0.7}\text{Ca}_{0.3}\text{MnO}_3$ (LCMO) films on perovskite substrates with different lattice constants [6] indicate that larger lattice distortion induced by the substrates gives rise to larger zero-field resistivity and larger negative magnetoresistance. In the present work we report our experimental investigations of the infrared properties of LCMO epitaxial films on various perovskite-based substrates: LaAlO_3 (LAO), SrTiO_3 (STO) and YAlO_3 (YAO). Infrared (IR) reflectivity spectra of single crystalline LAO, STO and YAO are also measured. Using the dielectric functions obtained directly from the bare substrate, we have fitted the measured reflectivity spectra of LCMO epitaxial films on the substrates by modeling the complex dielectric functions of bare LCMO. Our work indicates that the optical conductivity of LCMO and the observed Mn-O stretching and Mn-O-Mn bending phonon modes are strongly affected by the substrate-induced lattice distortion.

The LCMO epitaxial films are grown by pulsed laser deposition using a stoichiometric target of $\text{La}_{0.7}\text{Ca}_{0.3}\text{MnO}_3$, in 100 mTorr of oxygen. The temperature of the substrates is 700°C . The growth is followed by annealing in 1 atm. oxygen at 900°C for two hours, and the epitaxy of the films is confirmed by the x-ray rocking curves. The thickness of the films is 200 ± 10 nm. The lattice constants a , b and c ($c \perp$ sample surface) of all samples are determined using high resolution x-ray diffraction spectroscopy. The results are tabulated

in Table 1, As shown in Table 1, the lattice distortion induced by the substrates yields the mismatch lattice strain, defined as $(\Delta a_0/a_0)$, where a_0 is the lattice constant of the bulk perovskite, and Δa_0 is the difference between the lattice constant of the film and that of the bulk LCMO. The substrate-induced lattice strain has important effects on the optical Γ 1011011 modes. Therefore the infrared spectroscopy of films on different substrates can provide direct comparison of the phonon frequency shifts with the lattice strain, determined from x-ray diffraction measurements.

Near normal incidence reflectivity is measured (against a reference Al Mirror) with a Fourier-transform spectrometer in the entire IR spectral region 50-5000 cm^{-1} . The temperature of the sample is varied with a liquid He-cooled cryostat.

The large contribution of the substrate to the reflectance of LCMO thin films prevents direct derivation of the LCMO complex conductivity from the standard Kramers-Kronig transformations of the measured spectra. It is necessary to know the substrate dielectric function with high accuracy in order to model the optical spectra of the thin films. The complex dielectric functions of single crystalline LAO, STO and YAO are obtained by means of Kramers-Kronig (KK) analysis of the measured substrate spectra. For the analysis of the substrate spectra, we assume the constant reflectivity below 50 cm^{-1} and a single oscillator approximation above 5000 cm^{-1} . To avoid the KK transformation error due to the uncertainty in the extrapolation of the reflectivity spectra from zero to infinity, we perform analytical dispersion analysis of the measured spectra. A model based on the following factorized form of the complex dielectric function [7] is applied:

$$\hat{\epsilon}_s = \epsilon_{s\infty} \prod_j \frac{\omega^2 - \omega_{jz}^2 + i\gamma_{jz}\omega}{\omega^2 - \omega_{jp}^2 + i\gamma_{jp}\omega}. \quad (1)$$

The model has been successfully used to fit the IR reflectivity spectra of several perovskite oxides [8,9]. The adjustable parameters for the j th complex pole p and zero z in this description uniquely determine four phonon mode parameters for the j th transverse optical (TO)-longitudinal optical (LO) pair: the frequencies ω_{jT}, ω_{jL} and clamping terms γ_{jT}, γ_{jL} . The assumption of different parameters for the TO and LO modes is necessary when the

'1'0 and L.O modes have different phonon decay channels and different damping rates. The phonon mode parameters of the substrates and the high-frequency dielectric constant ϵ_∞ are initially evaluated from the KK analysis and then used as starting values for the least-squares fit of the reflectivity spectra to the factorized expression (1). By this means the complex refractive indices $\sqrt{\hat{\epsilon}_s} = \hat{n}_s = n_s + ik_s$ for the perovskite substrates are obtained and used in the two-layer (LCMO/substrate) modeling. Notice that good agreement between the optical quantities which yield the best fit to reflectivity data and those obtained from a KK analysis is observed above 150 cm^{-1} .

Near normal incidence reflectivity $R = |\hat{r}|^2$ of a film of thickness d on a semiinfinite substrate is related to the complex refractive indices of the film $\sqrt{\hat{\epsilon}_f} = \hat{n}_f = n_f + ik_f$ and of the substrate \hat{n}_s by the following equations for the reflectance amplitude \hat{r} [10]:

$$\hat{r} = \frac{\hat{r}_f + 1}{1 + \hat{r}_f}, \quad \Gamma = \frac{\hat{r}_f - \hat{r}_s}{\hat{r}_f \hat{r}_s + 1} \exp(2i\psi), \quad (2)$$

where

$$\hat{r}_f = \frac{1 - n_f + ik_f}{1 + n_f + ik_f}, \quad \hat{r}_s = \frac{1 - n_s + ik_s}{1 + n_s + ik_s}, \quad \psi = \frac{\omega}{c} d(n_f + ik_f).$$

The dielectric function of the film $\hat{\epsilon}_f$ is described in terms of the classical dispersion function which is the sum of contributions from a Drude term with plasma frequency ω_D and the damping parameter γ_D , and from Lorentzian oscillators with strengths S_j , frequencies ω_{fj} and damping parameters γ_{fj} for the j th mode

$$\hat{\epsilon}_f = \epsilon_{f\infty} - \frac{\omega_p^2}{\omega^2 + i\omega\gamma_D + \sum_j \frac{S_j}{\omega_{fj}^2 - \omega^2 - i\gamma_{fj}\omega}} \quad (3)$$

Once the substrate complex refractive indices \hat{n}_s is known, we use Eqs. (2)-(3) to fit the measured LCMO/substrate reflectivity spectra $R(\omega)$. Parameters for the optical phonons in $\text{La}_{1-x}\text{Sr}_x\text{MnO}_3$ crystals ($x=0.175$) [11] are selected as initial values for this least-squares fit.

Fig. 1a shows the reflectivity phonon spectra of LAO, YAO and STO at room temperature. The open circles represent the measured reflectivity spectra of LAO and S'1'0. the

solid curves are calculated by the fitting procedure based on Eq. (1). The fitting parameters thus obtained are listed in Table 11. The results for STO are almost the same as those previously reported by Kamaras *et al.* [9], although they did not resolve a weak phonon structure around 650 cm^{-1} . The parameters of the TO phonon modes determined for LAO agree well with those previously reported by Zhang *et al.* [12] and are derived by means of the classical dispersion analysis of the reflectivity spectrum [12]. The optical constants of the YAO substrate are obtained by the KK transformation, because many IR active phonons in YAO make the dispersion analysis more difficult.

The reflectivity phonon spectra of LCMO epitaxial films on the substrates are shown in Fig. 1 b. The open circles represent the experimental data, the solid curves were calculated by the fitting procedure based on Eqs. (2)-(3). The obtained fitting parameters are listed in Table 11. The Drude term in Eq. (3) is found to be negligible.

Figure 2 shows the optical conductivity spectra of bare LCMO, deposited on various substrates, obtained from $\tilde{\epsilon}_f$. There are three main phonon modes in the spectra: The Mn-O stretching mode observed around 550 cm^{-1} , the Mn-O-Mn bending mode around 350 cm^{-1} and the La(Ca)-site external mode, located around 160 cm^{-1} [1-3]. The bending mode is found to be split due to the orthorhombic distortion in LCMO. As shown in Fig. 2, the stretching and bending phonon modes shift significantly to lower frequencies, as the mismatch lattice strain (see Table I) increases. On the other hand, the external phonon frequency is nearly independent of the lattice constant. If the dependence of the phonon frequency on lattice constant is approximate] as $\omega \sim a^{-\alpha}$, the power α is roughly estimated to be 8 for the stretching mode and 5 for the bending mode. Similar strong a dependence of the stretching mode frequency is observed in layered cuprates and related materials [14]. This fact indicates that both of the highest frequency phonon modes may be strongly affected by the interaction with the electronic system, and the latter might also be modulated by the change in the Mn-O bond length and the Mn-O-Mn bond angle. It should be noted that line shapes of the phonon peaks in Fig. 2 are nearly independent of the lattice distortion induced by the substrates. It suggests that the LCMO epitaxial films under study are structurally

homogeneous structure throughout the entire film thickness.

In summary, an analysis of the reflectance of LCMO epitaxial films on various substrates with an extended range of lattice constants has been performed by taking into account the substrate contributions. Our results provide evidence for a strong dependence of the Mn-Mn bending and Mn-O stretching phonon mode parameters on the lattice distortion induced by the substrates. An extension of the present investigation to studying the variations of LCMO phonon modes with temperature and the analysis of the mid-IR reflectance and transmittance spectra may provide further understanding of the role of the lattice distortion and polaron conduction in the occurrence of the CMR effect in perovskite manganites.

A. V. Samoilov is supported by a Robert A. Millikan Prize Fellowship; N.-C. Yeh is sponsored by the National Aeronautics and Space Administration (NASA) and the Packard Foundation. Part of this work was performed by the Center for Space Microelectronic Technology, Jet Propulsion Laboratory, Caltech, under a contract with NASA.

*E-mail address: boris@issp.ac.ru

FIGURES

FIG. 1. Reflectivity phonon spectra Of LaAlO_3 , YAlO_3 , SrTiO_3 (a) and $\text{La}_{0.7}\text{Ca}_{0.3}\text{MnO}_3$ 011 the substrates (b) at 300 K. Open circles are experimental data and solid lines are the best fit of Eq. (1) (a) and Eqs. (2)-(3) (b) to the data. Solid curve for YAlO_3 is the measured reflectivity spectrum.

FIG. 2. Optical conductivity spectra of $\text{La}_{0.7}\text{Ca}_{0.3}\text{MnO}_3$ on various substrates calculated from $\hat{\epsilon}_f$ using the parameters of Table 3.

TABLES

TABLE I. The lattice constants and mismatch lattice strain determined from x-ray diffraction for $\text{La}_{0.7}\text{Ca}_{0.3}\text{MnO}_3$ (LCMO) epitaxial films on LaAlO_3 (LAO), YAlO_3 (YAO) and SrTiO_3 (STO) substrates at 300 K. For comparison, the lattice constants (in Å) for bulk LCMO are ($a/\sqrt{2} = 3.840$, $b/\sqrt{2} = 3.890$, $c/\sqrt{2} = 3.860$), LAO ($a = b = c = 3.792$), YAO ($a/\sqrt{2} = 3.662$, $b/\sqrt{2} = 3.768$, $c/\sqrt{2} = 3.685$), and STO ($a = b = c = 3.905$).

Compound	Lattice constant (Å)			Lattice Strain (%)		
	($a/\sqrt{2}$)	($b/\sqrt{2}$)	($c/\sqrt{2}$)	($\Delta a_o/a_o$)	($\Delta b_o/b_o$)	($\Delta c_o/c_o$)
LCMO/LAO	3.842	3.854	3.921	0.05	-0.93	1.58
LCMO/YAO	3.862	3.886	3.899	0.57	-0.10	1.01
LCMO/STO	3.881	3.927	3.845	1.07	0.95	-0.39

TABLE II. Best fit phonon parameters determined by Eq. (1) for LaAlO_3 (LAO) and SrTiO_3 (STO) at 300 K

LAO	ϵ_∞	4.2					
	ω_{JT}	183	427	494.4	651	680	
	γ_{JT}	3.9	6.4	1.7	22	65	
	ω_{jL}	277	596	494.5	743	687	
	γ_{jL}	4.3	9.9	1.6	10	70	
STO	ϵ_∞	5.2					
	ω_{JT}	92	175	443.5	544	635.1	710.1
	γ_{JT}	16	6.2	18.6	17	43	41
	ω_{jL}	171	476	443.8	793	635.2	710.8
	γ_{jL}	3.8	5.3	18.6	24	40	41

TABLE III. Best fit phonon parameters determined by Eqs. (2)-(3) for $\text{La}_{0.7}\text{Ca}_{0.3}\text{MnO}_3$ (LCMO) on LaAlO_3 (LAO), YAlO_3 (YAO) and SrTiO_3 (STO) substrates at 300 K.

	LCMO / LAO				LCMO / YAO				LCMO / STO			
ω_j	160	351	405	607.4	158	342	393	583	154	335	379	559
γ_j	53	51	52	71	64	73	46	76	59	83	30	65
S_j	670	792	511	832	707	805	447	761	671	854	259	669
ϵ_∞	8.6				9.0				8.4			

REFERENCES

- [1] A.J. Millis, P.B. Litterwood, and b.I. Shraiman, Phys.Rev.Lett. **74**, 5144 (1995); H. Roder, Jun Zang, and A.R.Bishop, Phys. Rev. Lett. **76**, (1 996); I. Solovyev, N. Hamada, and K. Terakura, Phys. Rev. Lett. **76**, 4825 (1 996).
- [2] S. Jin *et al.*, Science **264**, 413 (1 994); Appl.Phys.Lett. **66**, 3S2 (1995); Appl.Phys. Lett. **67**, 557 (1995).
- [3] H.Y. Hwang *et al.*, Phys. Rev. Lett. **75**, 914 (1995).
- [4] Y.X. Jia *et al.*, Phys. Rev. **1152**, 9147 (1995).
- [5] K. Khazen *et al.*, Phys. Rev. Lett. **76**, 295 (1996).
- [6] N. - C. Yeh *et al.*, to be published.
- [7] D.W. Berreman and F.C. Unterwald, Phys. Rev. **174**, 791 (1968)
- [8] F. Gervais *et al.*, Phys. Rev. **B47**, 8187 (1993).
- [9] H. Kamaras *et al.*, J. Appl. Phys. **78**, 1235 (1995)
- [10] L. D. Landau and E.M. Lifshitz, *Electrodynamics of continuous media* (Pergamon, oxford, New York, 1984).
- [11] Y. Okimoto *et al.*, Phys. Rev. Lett. **75**, 109 (1995).
- [12] Z.M. Zhang *et al.*, J. Opt. Soc. Am. **11**, 2252 (1994).
- [13] T. Arima and Y. Tokura, J. Phys. Soc. Japan **64**, 2488 (1995).
- [14] S. Tajima *et al.*, Phys. Rev. **B43**, 10496 (1991).

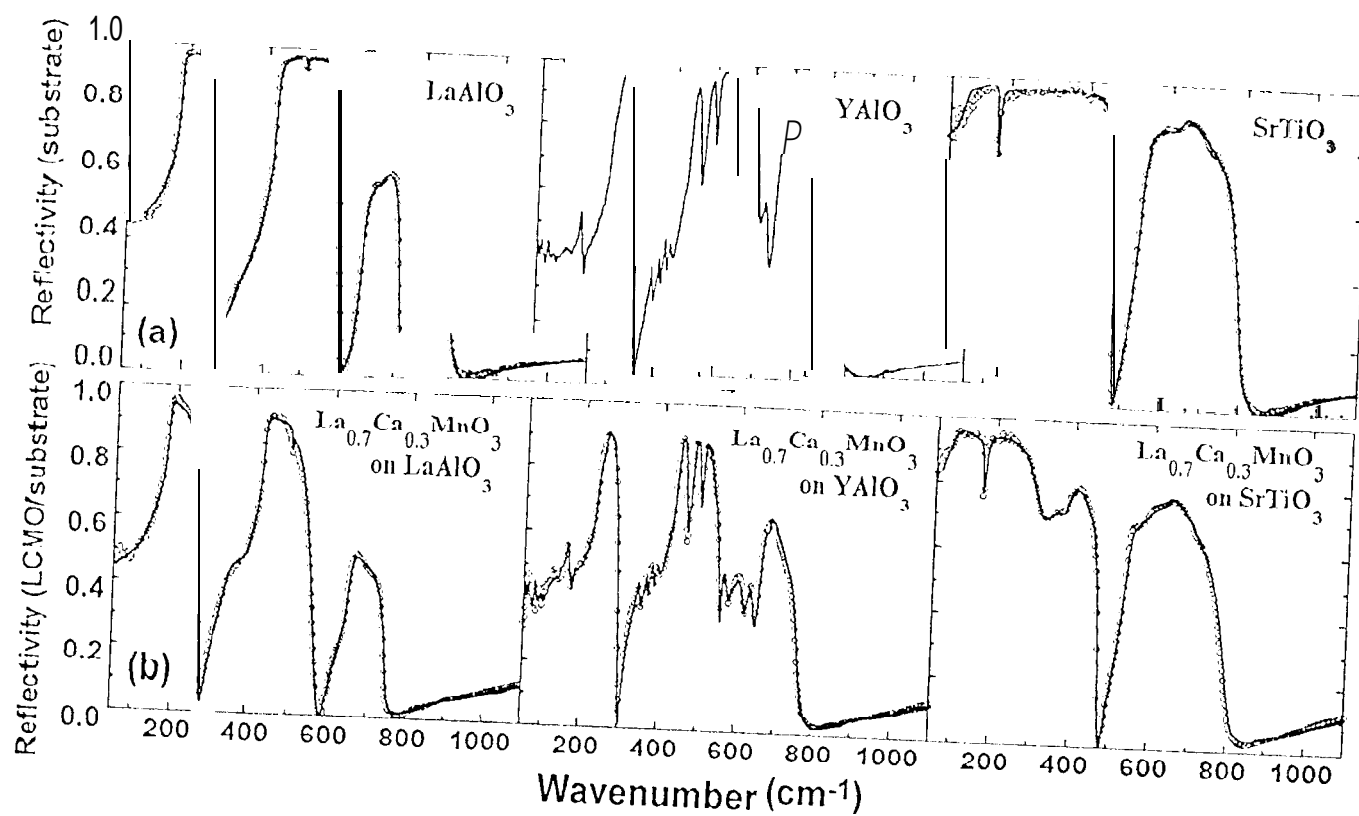


Fig. 1
Boris et al.

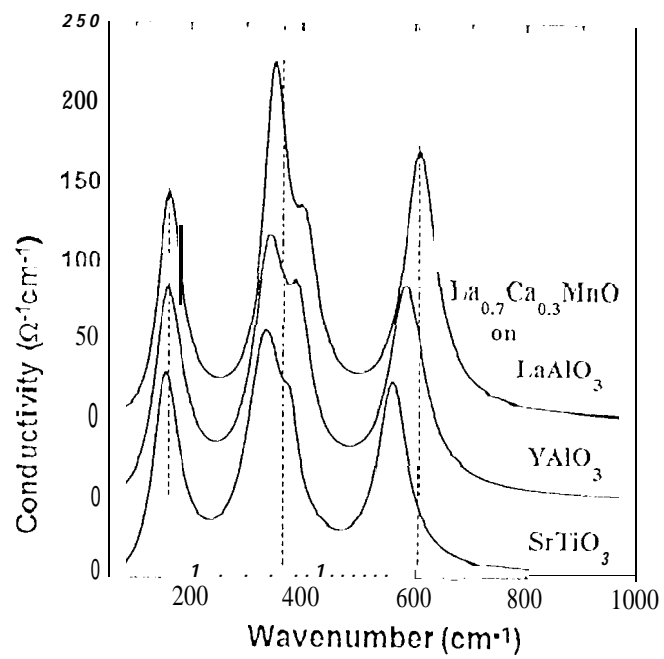


Fig.?,
Boris et al.